ELSEVIER

Biophysical Chemistry 120 (2006) 62 – 70

Biophysical Chemistry

http://www.elsevier.com/locate/biophyschem

Correlation between NQR parameters and residue size of aliphatic amino acids and their dimers

Ali Reza Ghaderi [a], Hassan Sabzyan [b,*], Nasser L. Hadipour [a]

[a] *Department of Chemistry, Tarbiat Modares University, Tehran 14115-175, Islamic Republic of Iran*
[b] *Department of Chemistry, University of Isfahan, Isfahan 81746-73441, Islamic Republic of Iran*

Received 22 August 2005; received in revised form 14 September 2005; accepted 14 September 2005
Available online 21 November 2005

Abstract

Nuclear quadrupole coupling constants (NQCC), χ, and asymmetry parameters, η, of ^{2}D, ^{14}N and ^{17}O nuclei have been calculated for aliphatic amino acids and their dimers using MP2/6-311++G** method to shed some light on the differences between the structural parameters in the aliphatic amino acids and their dimers. For this purpose, electric field gradient (EFG) at the sites of quadrupolar nuclei have been calculated and evaluated for each compound. A correlation is observed between the calculated NQCC parameters and the conformational structures of the compounds, showing that extraction of structural data from the NQR spectra might be promising. Our results showed that ^{17}O NQCC of terminal carboxylic acid and ^{14}N NQCC of the terminal amino groups are, respectively, the least and the most sensitive parameters to the variation of the size of the residue. It is found also that conformation of R (i.e. values of the dihedral angles) plays a very effective role in the determination of the values of the calculated NQCC parameters. Sensitivity of the NQR parameters to the changes in the conformational structure is significantly greater (nearly 20-fold) than that to the changes in the other structural parameters such as bond lengths.

Keywords: Ab initio; NQCC; Aliphatic amino acid; Dimer; MP2/6-311++G**

1. Introduction

Investigation of the conformational details of biological macromolecules is important in the understanding of their functions. Therefore, determination of the structure of biomolecules in aqueous solutions, as well as calculation of their spectral properties, is currently the problem of great interest [1–3]. Most of what is known about protein conformation has been obtained from water soluble proteins. Many such proteins are relatively easy to crystallize and therefore can also be studied by X-ray diffraction methods [4]. However, the relevance of the molecular structures in their crystalline phase for the biological molecules in aqueous solution is often questioned. Experimental approaches such as nuclear magnetic resonance (NMR), nuclear quadrupole resonance (NQR) and Raman spectroscopies allow us to complement the information obtained from X-ray crystallographic studies.

NMR has been used for some 45 years to study atomic arrangement, chemical bonding and structural grouping in crystalline forms [5]. Solid-state nuclear magnetic resonance has had a major role in the elucidation of protein compositions. Recently, structural characterization of 15 amino acid transmembrane dimers in fully hydrated lipid bilayers carried out using solid state NMR demonstrated that this approach is capable to contribute to the structural biology field [6,7].

NQR spectroscopy has more recently increased the resolution and accuracy of the experimental results obtained in the measurements on peptides and proteins [8–13]. The driving force behind this trend is the need for a new approach to solve protein structure in anisotropic environments where both crystallography and solution NMR methods fail. The parameters, which could be measured experimentally by NQR spectroscopy, are the NQR frequency (ν_Q) and nuclear quadrupole coupling constant (NQCC). In NQR spectroscopy, the interaction between nuclear electric quadrupole moments of quadrupolar nuclei (having spin $I>1/2$) with the local molecular electric field gradient (EFG) has the characteristic role [14,15]. The EFG at a nucleus in molecular environment is

* Corresponding author. Tel.: +98 311 793 2749; fax: +98 311 668 9732.
E-mail address: sabzyan@sci.ui.ac.ir (H. Sabzyan).

0301-4622/$ - see front matter © 2005 Elsevier B.V. All rights reserved.
doi:10.1016/j.bpc.2005.09.023

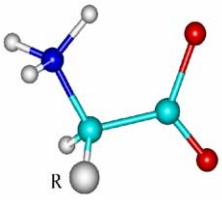

Monomer	R	Dimer
Gly	H	**Gly-Gly**
Ala	CH_3	**Gly-Ala**
Val	$CH(CH_3)_2$	**Gly-Val**
Ile	$CH_2CH(CH_3)_2$	**Gly-Ile**
Leu	$CH(CH_3)(C_2H_5)$	**Gly-Leu**

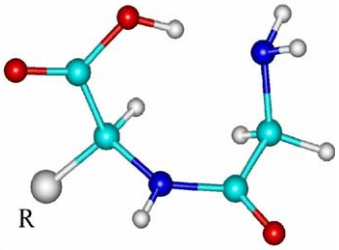

Fig. 1. The amino acid monomers and dimers studied in this work.

a one-electron property and can be obtained with a reasonable effort using ab initio computations. Since, it involves only the ground state wave function, calculation of the EFG should be easier and faster than the calculation of the NMR chemical shifts. Therefore, theoretical efforts needed to devote to the interpretation of NQR spectroscopy are less than that of NMR spectroscopy [16,17].

In the study of small protein fragments reported by Torrent et al., the ^{17}O and ^{14}N NQCC values and their asymmetry parameters were calculated theoretically to distinguish between the two secondary structures, α-helix and β-sheet, of proteins. In this work, it has been stated that the calculated NQCC value for the ^{17}O atom of the peptide bond in proteins depends on the specific conformation of the backbone. This parameter is observably different between α-helices and β-sheets. Hence, protein conformation may be identified through analysis of the ^{17}O NQR parameter [18].

The components of the EFG tensor are defined in its principal axis system and are ordered as follows:

$$|q_{ZZ}| \geq |q_{YY}| \geq |q_{XX}|$$

The nuclear quadrupole coupling constant, abbreviated as NQCC and denoted by χ, of a given quadrupolar nucleus is given by

$$\chi = \frac{e^2 q_{ZZ} Q}{h}$$

where e is the charge of electron, Q is the nuclear electric quadrupole moment of the nucleus and h is the Plank's constant.

The NQCC parameter is a measure of the interaction between the nuclear quadrupole moment and the EFG at the quadrupole nucleus site due to the nonspherical and noncylindrical (anisotropic) charge distribution in the system. Such interaction can be measured either in the gas phase (using microwave spectroscopy) or in the solid phase (mostly by NQR spectroscopy).

Asymmetry parameter, η, which is a measure of the deviation of the charge distribution from axial symmetry, is defined as:

$$\eta = \left| \frac{q_{YY} - q_{XX}}{q_{ZZ}} \right|$$

When η is equal or close to zero (i.e. when $q_{XX} \cong q_{YY}$), for example, it definitely points to a cylindrical symmetry in the electron density distribution around the quadrupolar nuclei [19].

Since, q_{ii} elements (the diagonal components of the EFG tensor, where $i = X$, Y and Z) correspond to the quality of the charge distribution in molecule, therefore NQCC and η values are extremely sensitive to atomic and chemical bonds arrangements and are excellent probes for the identification of bonding conformations and structural groupings in chemical compounds.

Considering that foregoing experimental methods are not applicable to all problems, use of theoretical methods is crucial to supplement the information obtained from experimental measurements. However, it may be difficult to implement all theoretical approaches directly for large systems (such as proteins). Therefore, determination of the properties of the building units as a model (such as amino acids) will be useful.

In this work aliphatic amino acids (Gly, Ala, Val, Leu and Ile) and their dimers (Gly–Gly, Gly–Ala, Gly–Val, Gly–Leu and Gly–Ile) are studied as benchmarks for the study of proteins (Fig. 1). We try to examine the ability of the NQR, as a reliable method, to distinguish different positions of a specific amino acid (for example, glycine) in a protein structure, which might appear identical or similar in the other spectroscopic methods. In this line, variation of the ^{14}N, ^{2}D and ^{17}O NQR parameters in the selected amino acids and their dimers has been studied.

2. Computational details

Gradient optimization techniques were employed to optimize geometry of molecules at the HF, MP2 and B3LYP levels of theory using 6-31G*, 6-31G**, 6-311G**, 6-311+G** and 6-311++G** basis sets. All ab initio calculations were performed using the GAUSSIAN98 package [20]. To evaluate and ensure the optimized structures of the molecules, frequency calculations were carried out using analytical second derivatives. In all cases only real frequencies were obtained for the optimized structures. At first, calculations were carried out on glycine. The results are tabulated in Table 1.

The data reported in Table 1 shows that HF method predicts more stability for the zwitterion form compared to the non-ionized form. While, MP2 and B3LYP methods predict that the non-ionized form of the glycine amino acid is more stable, and

Table 1
Nuclear quadrupole coupling constants (NQCC),χ, and asymmetry parameters calculated for the ^{2}D, ^{14}N and ^{17}O nuclei and the gas phase electronic energies E_{el} (in Hartree) for glycine using different levels of theory and basis sets, starting with two different initial structures

Nucleus	^{2}D		^{14}N		^{17}O1		^{17}O2		$-E_{el}$
Basis set	χ (kHz)	η	χ (MHz)	η	χ (MHz)	η	χ (MHz)	η	
a) RHF: initially non-ionized									
6-31G*	304.7	0.1107	4.9335	0.1500	8.6508	0.5497	10.0880	0.1349	741.721
6-31G**	313.9	0.1217	4.9787	0.1314	8.6579	0.5488	10.0790	0.1329	741.756
6-311G**	320.8	0.1182	5.4632	0.1586	8.1851	0.5225	10.3340	0.2688	741.939
6-311+G**	320.7	0.1192	5.2354	0.1762	8.9549	0.4921	10.2220	0.2430	741.966
6-311++G**	320.6	0.1193	5.2326	0.1761	8.9530	0.4916	10.2200	0.2431	741.966
b) RHF: initially zwitterions									
6-31G*	265.2	0.0076	5.7888	0.4980	7.8656	0.5756	8.5527	0.3342	741.840
6-31G**	267.1	0.0071	6.2719	0.6194	7.8446	0.5777	8.5667	0.3304	741.885
6-311G**	274.3	0.0095	5.7538	0.4447	8.0847	0.4949	8.7559	0.2187	742.065
6-311+G**	273.9	0.0086	5.2304	0.4498	8.3187	0.4604	8.7514	0.2267	742.086
6-311++G**	273.6	0.0087	5.3080	0.4394	8.3155	0.4591	8.7537	0.2276	742.086
c) RB3LYP: initially non-ionized									
6-31G*	221.6	0.1258	4.5412	0.1543	7.4197	0.5551	9.2812	0.0517	746.026
6-31G**	226.1	0.1364	4.5633	0.1466	7.3867	0.5576	9.2715	0.0494	746.064
6-311G**	244.3	0.1266	5.1743	0.1753	8.1023	0.5251	9.6654	0.1813	746.275
6-311+G**	246.7	0.1261	4.9438	0.2029	7.8338	0.4932	9.4976	0.1465	746.305
6-311++G**	246.6	0.1265	4.9414	0.2028	7.8257	0.4938	9.4962	0.1463	746.296
d) RB3LYP: initially zwitterions									
6-31G*	221.4	0.1259	4.5426	0.1545	7.4161	0.5554	9.2763	0.0515	746.026
6-31G**	226.2	0.1364	4.5637	0.1467	7.3878	0.5582	9.2707	0.0500	746.064
6-311G**	244.3	0.1266	5.1753	0.1754	8.1025	0.5252	9.6655	0.1813	746.275
6-311+G**	247.0	0.1260	4.9550	0.2014	7.8346	0.4976	9.4965	0.1485	746.305
6-311++G**	246.6	0.1266	4.9549	0.2017	7.8206	0.4981	9.4904	0.1476	746.305
e) RMP2: initially non-ionized									
6-31G*	222.4	0.1584	4.7746	0.1503	8.4162	0.6535	10.3990	0.0273	743.865
6-31G**	236.0	0.1708	4.7812	0.1358	8.3753	0.6545	10.3960	0.0309	743.986
6-311G**	242.0	0.1677	5.2582	0.1601	8.7946	0.6263	10.6320	0.1481	744.319
6-311+G**	243.3	0.1636	5.1045	0.1777	8.6386	0.5987	10.5180	0.1202	744.360
6-311++G**	242.9	0.1638	5.1049	0.1776	8.6283	0.5980	10.5130	0.1191	744.361
f) RMP2: initially zwitterions									
6-31G*	216.1	0.1601	4.7909	0.1593	8.2761	0.6450	10.2670	0.008	743.864
6-31G**	228.6	0.1733	4.7974	0.1437	8.2239	0.6454	10.2620	0.0027	743.985
6-311G**	236.5	0.1694	5.2579	0.1674	8.6672	0.6187	10.5150	0.1271	744.319
6-311+G**	239.6	0.1643	5.1110	0.1829	8.5527	0.5906	10.4300	0.1034	744.359
6-311++G**	242.8	0.1638	5.1040	0.1776	8.6284	0.5977	10.4310	0.1036	744.361

thus when starting with a zwitterion form, proton transfer occurs during the optimization procedure (Fig. 2). This comparative behavior can be attributed to the electronic correlation energy taken into account in the post-SCF methods only. In the electronic structure theories of atoms and molecules, based on both traditional molecular orbital (MO) theories and the developing density functional theories (DFT), the electron correlation is one of the most important concepts. The central issue in quantum chemical computations is how to take electron–electron correlation into consideration. A HF-SCF wave function takes into account the interaction between electrons only in the form of an average field neglecting the instantaneous interactions between electrons. Therefore, in HF method, the electron correlation effect is not exactly and correctly estimated, while, in MP2 and B3LYP methods, instantaneous interactions between electrons are taken into account appropriately. Therefore, MP2 and B3LYP results are more reliable [21].

The instability of the zwitterion structures of amino acids in the gas phase has been previously studied for glycine in a number of detailed ab initio electronic structure investigations [22,23]. Furthermore, in several other studies, alanine has been treated in its non-ionized form [24,25]. It is well known that amino acids exist as zwitterions in the crystalline state as well as in the aqueous solution because of the stabilizing effects of the electrostatic, polarization and hydrogen-bonding (HB) interactions with the solvent molecules [26,27]. In the gas phase, however, where these intermolecular interactions are absent, amino acids exist in their non-ionized forms [28,29]. Formation of zwitterion in aqueous solutions occurs via the ionization of the carboxylic acid and amino groups. The resulting charged groups,

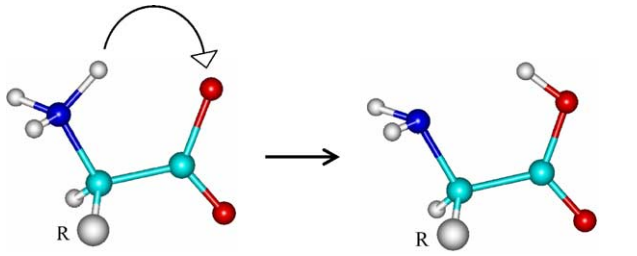

Fig. 2. Interconversion of the zwitterionic and non-ionized structures of amino acids via proton transfer.

$-COO^-$ and $-N^+H_3$, strongly interact with each other and with their environments.

It is now interesting to know why proton transfer takes place during the geometry optimization processes in the MP2 and B3LYP methods. One probable suggestion is that in the restricted methods (RMP2 and RB3LYP), some spin and symmetry adapted excited Slater determinants that contribute to further stabilization of zwitterionic form are ignored. These determinants correspond mainly to the HOMO (highest occupied molecular orbital) of the molecule. The method in which these contributions are considered in the evaluation of molecular electronic energy and the optimized geometry is known as configuration interaction (CI). The CI computations on these systems are beyond the scope of this study. However, in order to examine this reflection at a lower level, the optimized structures obtained for the zwitterionic form of glycine from both restricted (RMP2 and RB3LYP) and unrestricted (UMP2 and UB3LYP) methods were compared. The optimized final structures obtained from both sets of restricted and unrestricted methods were found to be very similar. The identical electronic energies obtained in these couple sets of calculations also establish this point (Table 2). Therefore, this hypothesis (limitations of the restricted methods in the characterization of the optimized structure) is not true and thus the non-ionized form can be regarded as the stable form of amino acids in the gas phase.

In order to examine the proton transfer on all of the selected amino acids and their dimers, the optimization procedures were started from the zwitterions as the initial forms. It was found that for all of the selected amino acids and their dimers, proton transfer occurs at MP2 and B3LYP levels of theory, implying that all of these species exist in their non-ionized forms.

Table 2
Comparison of the electronic energy E_{el} (in Hartree), the nuclear quadrupole coupling constant χ, and asymmetry parameter for ^{2}D, ^{14}N and ^{17}O nuclei of glycine calculated with restricted and unrestricted methods using 6-311++G** basis set starting from the zwitterionic structures

Computational method		RMP2	UMP2	RB3LYP	UB3LYP
$-E_{el}$ (Hartree)		744.3608	744.3605	746.3052	746.3052
^{2}D	χ (kHz)	242.8	239.6	246.6	246.6
	η	0.1638	0.1647	0.1266	0.1265
^{14}N	χ (MHz)	5.1040	5.1127	4.9549	4.9546
	η	0.1776	0.1826	0.2017	0.2018
^{17}O	χ (MHz)	8.6284	8.5446	7.8206	7.8185
	η	0.5977	0.5906	0.4981	0.4967

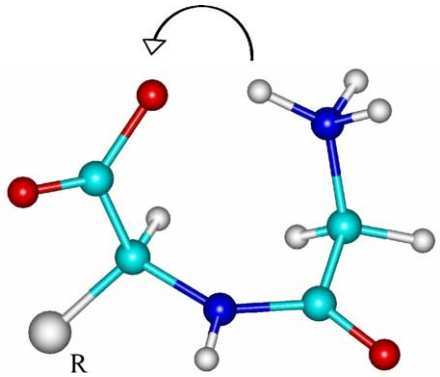

Fig. 3. Proton transfer from the terminal amino group to the carboxylic group in amino acid dimers (α conformer).

Starting from the end–end zwitterionic form for dimers, three types of proton transfer are possible. The first type is the migration of proton from terminal amino group to the terminal carboxylic group (Fig. 3). Other types of migration can occur just by a change in the two dihedral angles in the dimer (Fig. 4). This change can result in either a second proton transfer from the terminal amino group to the oxygen of the peptide bond or a third proton transfer from the peptide bond to the terminal carboxylic acid group. Comparison between electronic energies of the two possible conformers of Gly–Ala dimer (see Figs. 3 and 4) shows that the α conformer is 30.02 kJ/mol more stable than the β conformer. Therefore, α conformer of dimers was considered as initial structure in the subsequent computation steps.

To select the most suitable method for computing the NQR parameters, the calculated parameters at various levels of theory are compared with experimentally measured NQR parameters for glycine (Table 1). In general, the data in Table 1 show that the NQCC values increase upon the increase of the size of the basis set used. It means that the greater basis set provides greater space for interaction between nuclear quadrupole moments of the quadrupolar nuclei and the local electric field gradient. Inspection of NQCC data reported in Table 1 indicates that for the calculation of NQR parameters in amino acids, the agreement observed between the experimentally measured values of ^{2}D NQCC and the MP2/6-311++G** calculated values is better than that observed for the calculated

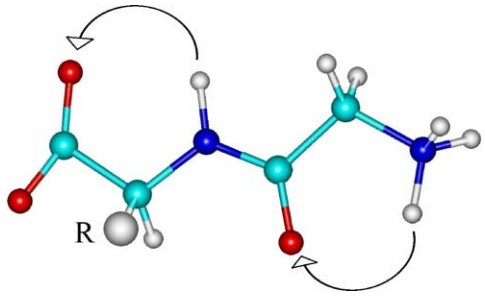

Fig. 4. Two synchronous proton transfers in amino acid dimers (β conformer).

values by B3LYP/6-311++G** method [30–32]. This is why MP2 is considered as a more suitable method.

Furthermore, calculated values of ^{17}O NQCC reported in Table 1 show that ^{17}O1 NQCC is smaller than ^{17}O2 NQCC due to the participation of the O1 (recipient of the migrating proton) nonbonding electrons in the bonding interactions with the migrating proton. Therefore, the NQCC values of the atoms containing nonbonding electrons could be considered as a criterion in the determination of the nonbonding electron sharing in bonding interactions with neighboring atoms. If a suitable reference is set, it is then possible to scale electron-sharing of different atoms containing nonbonding electrons provided that at least one quadrupolar isotope exists for each element.

For the calculation of the NQCC parameters, the most recent values of electric quadrupole moments reported in Ref. [33] are used.

3. Results and discussion

EFG calculations were carried out on the MP2/6-311++G** optimized structures of the selected amino acids and their dimers. The results are reported in Tables 3–5. As mentioned previously, our aim is to determine the effect of structure on the NQCC parameters. It should be noted here that in this work, it is not intended to put emphasis on the calculated values of NQCC parameters. It is rather intended to develop a methodology by which the measured NQCC values can be used to figure out the sequence and secondary structures of proteins, or to refine the structures already obtained by other techniques.

Different parts of the selected amino acids and their dimers such as alpha-hydrogen (H_α), carboxylic and terminal amino groups, as well as the components of the peptide bond in dimers have been probed for this study (see Fig. 5). Calculated values of NQCC and asymmetry parameters are listed in Table 3. A detailed analysis of the calculated values of EFG has been carried out and the results are classified as follows:

A) If the last NQCC value in the **A1** series (the **A1** ^{2}D NQCC in Leu) is set aside, the remaining ^{2}D NQCC values show a decreasing trend which can be attributed to the change in the R group. But for the strange value reported for the ^{2}D NQCC of Leu, the C–H(**A1**) bond distance can be considered to be responsible in the observed trend. If this C–H bond distance increases, the ^{2}D NQCC should be decreased due to the decrease in the charge density on the H atom. The C–H(**A1**) bond distances in Ile and Leu deduced from the optimized structures are 1.1005 and 1.0959 Å, respectively (within a ±0.0005 Å accuracy of the calculated bond length [20]). The longer bond distance in Ile is just due to the more effective interaction between this H atom and the corresponding R group. As can be seen from the optimized structures of the Ile and Leu, the isobutyl R group in Leu is aligned closer to the H(**A1**) atom, while the 1-methylpropyl R group in Ile is oriented far from the H(**A1**) atom. Therefore,

Table 4
The optimized values of the inter-atomic distances R_{O-N} (between terminal carboxylic oxygen and terminal amino nitrogen atoms), R_{O-H} (between the terminal carboxylic oxygen and acidic hydrogen atoms) and R_{N-H} (between the acidic hydrogen and terminal amino nitrogen atoms), and the calculated NQCC values in the selected amino acid monomers and dimers

Molecule	R_{O-N} (Å)	R_{N-H} (Å)	R_{O-H} (Å)	χ_O (**C**)	χ_N (**D**)	χ_H (**B**)
Gly	2.6175	1.9054	0.9807	8.6284	5.1040	242.8
Ala	2.6064	1.9032	0.9805	8.6520	5.0542	242.7
Val	2.5783	1.8826	0.9805	8.7125	5.1511	242.3
Ile	2.5904	1.9051	0.9796	8.7730	5.1488	235.8
Leu	2.5902	1.8657	0.9726	8.8196	5.1134	236.5
Gly–Gly	2.7680	1.7759	0.9926	9.0139	4.8817	197.6
Gly–Ala	2.7773	1.7883	0.9919	9.0421	4.8870	199.8
Gly–Val	2.7984	1.8149	0.9906	9.0479	4.8929	204.6
Gly–Ile	2.7988	1.8135	0.9913	9.0580	4.8939	202.2
Gly–Leu	2.8727	1.9833	0.9889	9.0421	4.8942	206.2

Table 3
The calculated values of nuclear quadrupole coupling constant χ, and asymmetry parameter η for different nuclei of the selected amino acid monomers and dimers studied in this work using MP2/6-311++G** level of theory

Nucleus	Parameter	Gly	Ala	Val	Ile	Leu	Gly–Gly	Gly–Ala	Gly–Val	Gly–Ile	Gly–Leu
^{2}D (**A1**)	χ (kHz)	202.2	198.0	193.3	193.3	197.7	201.8	200.1	197.2	197.7	195.1
	η	0.0527	0.0301	0.0332	0.0338	0.0402	0.0604	0.0499	0.0461	0.0444	0.0451
^{2}D (**A2**)	χ(kHz)	–	–	–	–	–	200.9	200.7	200.4	200.7	200.3
	η	–	–	–	–	–	0.0373	0.0383	0.0396	0.0377	0.0508
^{2}D (**B**)	χ (kHz)	242.8	242.7	242.3	235.8	236.5	197.6	199.8	204.6	202.2	206.2
	η	0.1638	0.1618	1653	0.1639	0.1652	0.2118	0.2071	0.2063	0.2033	0.1519
^{17}O (**C**)	χ(MHz)	8.6284	8.6520	8.7125	8.7730	8.8196	9.0139	9.0421	9.0479	9.0580	9.4205
	η	0.5977	0.5973	0.5988	0.6130	0.6780	0.4519	0.4610	0.4966	0.4608	0.7245
^{14}N (**D**)	χ (MHz)	5.1040	5.0542	5.1511	5.1488	5.1134	4.8817	4.8870	4.8929	4.8939	5.2942
	η	0.1776	0.1475	0.1348	0.1362	0.1360	0.2091	0.2053	0.2003	0.2081	0.1720
^{2}D (**E**)	χ (kHz)	273.8	270.7	269.3	269.3	271.0	263.0	263.0	262.8	263.0	263.5
	η	0.1658	0.1658	0.1568	0.1574	0.1620	0.1422	0.1422	0.1422	0.1423	0.1675
^{2}D (**F**)	χ (kHz)	–	–	–	–	–	265.9	263.6	263.3	263.1	253.1
	η	–	–	–	–	–	0.2141	0.2152	0.2107	0.2082	0.1953
^{14}N (**G1**)	χ (MHz)	–	–	–	–	–	5.1856	5.1336	5.1890	5.0541	4.4633
	η	–	–	–	–	–	0.1336	0.0980	0.0909	0.1151	0.2244
^{17}O (**G2**)	χ (MHz)	–	–	–	–	–	10.8440	10.8270	10.8340	10.8300	10.4540
	η	–	–	–	–	–	0.0328	0.0430	0.0433	0.0393	0.0312.26

Table 5
The optimized values of the peptide group N–H bond length (in Å) and the related ^{14}N(G1) and ^{2}H(F) NQCC values, $\chi(^{14}N)$ in MHz and $\chi(^{2}H)$ in kHz respectively, obtained for the aliphatic amino acid dimers

Dimer	R_{N-H}(Å)	$\chi(^{14}N)$/MHz	$\chi(^{2}H)$/kHz
Gly–Gly	1.0135	5.1856	265.9
Gly–Ala	1.0150	5.1336	263.6
Gly–Val	1.0152	5.1890	263.3
Gly–Ile	1.0156	5.0541	263.1
Gly–Leu	1.0162	4.4033	253.1

See Fig. 5 for numbering scheme.

neglecting the Leu case, the calculated ^{2}D NQCC values for monomers show a decreasing trend for the H(**A1**) series, with the size of the R group.

In the dimers, two types of alpha-hydrogens exist; one from Glycine and the other from the other monomer (i.e. Glycine, Alanine, Valine, Leucine and Isoleucine amino acids). The extent of the variation of the NQCC with the size of the R group is smaller for the dimers. Structural strain forces the R group to be aligned far from H_α in the dimers. Therefore, the interaction between R and the H_α in the dimers is weaker than that in the monomers. Also, the NQCC data for the H_α in the dimers show that different R groups have no effect on the calculated values of NQCCs for H_α in the glycyle part. The **A2** proton and R group are aligned in the opposite directions due to the structural strain and thus have long distance (at least, certainly longer than a direct chemical bond by a factor of 2) interaction. This means that the **A2** proton is oriented in the inner section of the dimer molecule, while the R group is aligned in the outer section and these two species have no significant effect on each other. The calculated NQCCs of the **A1** and **A2** protons also establish this point. Based on these results, any geometry suggested for the dimer may be confirmed by analyzing the calculated NQCCs of the **A1** and **A2** protons. The NQCC value of the **A2** proton is rather constant, while the NQCC value of the **A1** proton is changed due to the dissimilar R groups. This change is even larger for larger R groups. On the other hand, it would be claimed that our aim in this section is to determine how the R group is aligned in the dimer molecule. This is reflected in the difference between the calculated values of NQCC for the **A1** and **A2** protons.

B) The computational results showed that the acidic proton migrates from the terminal amino group to the terminal carboxylic group and the amino acid molecules revert to the non-ionized form. It should be noted here again that the proton transfer scheme shown in Fig. 4 has been adopted.

In this part, the NQCC of the migrating ^{2}D are discussed. The data in Table 3 show that for both monomers and dimers, the ^{2}D NQCC changes with the R group, however a certain trend could not be observed. It seems that with an increase in the size of the R group, ^{2}D NQCC decreases for monomers while increases for dimers.

According to the literature, the terminal amino group hydrogen atoms take part in H-bonding with the neighboring groups [34–38]. The H-bond interaction has a significant role in the determination of the NQCC values. Therefore, for accurate description of the ^{2}D NQCC of the terminal amino group, the H-bond interaction should be taken into account. What is obvious from the calculated NQCC values is that the variation of the ^{2}D NQCC value is just due to the variation of the R group. Because of the larger steric effects in dimers (as compared to that in monomers), the larger R group is aligned farther from other species. Hence, the charge density on ^{2}D(**B**) in dimers is higher than that in monomers. Consequently, the corresponding ^{2}D(**B**) NQCC values in dimers are larger than those in monomers.

The values and the symmetry of the charge densities around the quadrupolar nuclei control the NQR parameters. Different types of the direct and indirect chemical bonding and interactions through space, such as hydrogen bonding or repulsion, determine values and the symmetry of the charge distribution in all points of a molecule including the quadrupolar nuclei sites. These factors have a variety of combination effects which analysis is sometimes difficult. The collective effects of the interactions through space are termed as steric effects which in the present case arise from different R groups. Therefore, it would be stated that variation in the inter-atomic distances and the corresponding NQCC values are almost mainly due to the variations of the steric effects of the R groups.

Table 4 lists the inter-atomic distances N–H, N–O and O–H between the transferring proton or deuteron, nitrogen atom of the terminal amino group and the oxygen atom of the terminal carboxylic group (recipient of the transferring proton or deuteron) in the optimized structures of the selected amino acid monomers and dimers obtained at the MP2/6-311++G** level of theory. In monomers, the N–H, N–O and O–H distances decrease with increasing the size of the R group. This shows a stronger interaction between these parts and the larger R group. This can justify the trend observed for ^{2}D NQCC in monomers. While in dimers, the increase in the size of the R

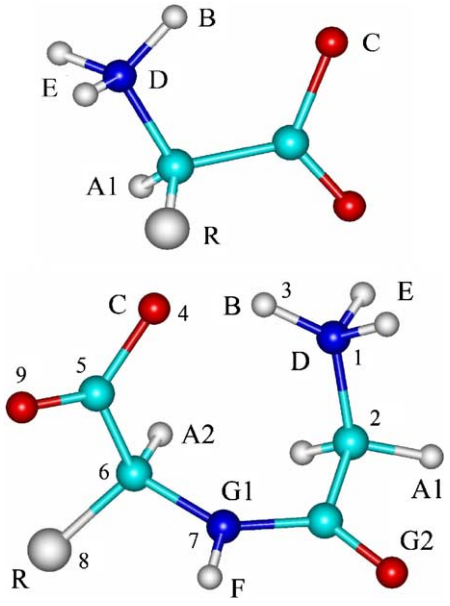

Fig. 5. The components of the amino acid monomers (top) and dimers (bottom) considered in this work as indicators.

Table 6
NBO analysis of the through space (remote) interaction between the R group and the neighboring atoms in Gly and Gly–Gly molecules

Molecule	Donor	Acceptor	$E(2)$	ΔE	F_{ij}
Gly	BD C_1-H_6	BD* C_3-O_4	3.00	0.96	0.050
	BD C_1-H_6	BD* C_3-O_5	2.83	1.37	0.056
	BD C_1-H_7	BD* C_3-O_4	6.4	0.96	0.072
	BD C_1-H_7	BD* C_3-O_5	0.91	1.37	0.032
Gly–Gly	BD $C_{12}-H_{13}$[a]	BD* $C_{15}-O_{17}$[a]	2.26	1.67	0.055
			3.81	0.95	0.055
	BD $C_{12}-H_{14}$	BD* $C_{15}-O_{16}$	4.89	1.38	0.074

$E(2)$: hyper-conjugation energy from the second order perturbation approach.
ΔE: the difference in energy between the interacting orbital.
F_{ij}: the Fock matrix element between the natural bond orbitals i and j.
[a] Two hyper-conjugative interactions are possible between these two natural bonds.

group increases the distance between the N and O atoms of the peptide bond. The observed trends of the ^{14}N(**G1**) and ^{2}D(**F**) NQCC values can be simply interpreted based on the length of the peptide bond. Upon increasing the N–H bond length which is associated with a decrease in the charge density around the N atom, the N–H bond orbital is expanded and its difference with the nonbonding electron orbitals is reduced. In other words, asymmetry of the charge density around the N atom decreases with increasing the N–H bond length and thus, the χ_N value is decreased. The χ_H values show the same trend as the symmetry of the charge density on the hydrogen atom is decreased with increasing the N–H bond length. The data reported in Table 5 confirm this trend.

C) In both monomers and dimers, the ^{17}O NQCC for the oxygen atom of the carboxylic group (which receives the transferring proton or deuteron) increases when the size of the R group increases. This can be attributed to the decrease in the interaction between R group and this oxygen atom. Such a conclusion about the ^{17}O NQCC is quite crude. Considering the well-known trend of hydrogen bond formation between the oxygen atom in the caboxylate $-CO_2^-$ group and one of the hydrogen atoms in the $-N^+H_3$ group (or similarly of the hydrogen atom in the peptide amino group), a strong interaction between the carboxylate and other groups in amino acids is expected [39–41]. Hydrogen bonding has a larger effect on the anisotropy of the charge distribution in the carboxyl group as compared with other interactions. A linear correlation between q_{ZZ} at the C–O–H oxygen site and q_{ZZ} at the C⌒O...H oxygen site (in a C–O–H...O⌒C hydrogen bond) is observed, which makes the assignment of the complex ^{17}O NQR spectra possible in these systems. Using the obtained relationship between q_{ZZ} and the O–O inter-atomic distance ($R_{O...O}$) of the hydrogen bond, extracting structural data from the ^{17}O NQR spectra becomes possible for both oxygen sites [42]. In a ^{17}O–H group, as well as in a ^{17}O...H hydrogen bond, the rather strong proton-oxygen magnetic dipole–dipole interactions produce a fine structure in the ^{17}O NQR spectrum which may be used for the determination of the O–H distance and the orientation of the O–H bond in the principal axes frame of the EFG tensor [43]. The values of the EFG tensor elements at the oxygen site depend mainly on the electric charge distribution in the chemical bonds formed by oxygen [44]. Therefore, description of the ^{17}O NQCC is dominantly related to the hydrogen-bond (H-bond) involving this oxygen atom.

An NBO analysis [45–50] carried out on the representative monomer and dimer molecules reported in Table 6 confirms this point. As can be seen from these results, hyper-conjugation interaction between the σ_{C-R} bond (as the donor orbital) and the σ^*_{C-O} bond (as the acceptor orbital) in the Gly monomer is stronger than that in Gly–Gly dimer. It is noticeable that these hyper-conjugative stereoelectronic interactions can provide electron density to the electron deficient centers or withdraw from electron rich centers. In this case, a better hyper-conjugative $\sigma_{C-R} \rightarrow \sigma^*_{C-O}$ interaction caused the charge density on the oxygen atom to be increased, and consequently, its NQCC value to be decreased. A reversed trend is expected for $\sigma_{C-O} \rightarrow \sigma^*_{C-R}$ interaction.

Since, in this work, only isolated single molecules (monomers and dimers) are considered, intermolecular hydrogen bonding is not a determining factor. Therefore, increasing the ^{17}O NQCC with the size of the R group observed in the present study can only be attributed to the decreasing interaction between the R group and this oxygen atom.

The optimum dihedral angles, which give us an idea about the steric status of the R group, related to the ^{17}O(**C**) and ^{14}N(**D**) atoms are given in Table 7. All dihedral angles clearly show that compared to Gly–Ile, the R group in Gly–Leu dimer is farther from the ^{17}O(**C**) and ^{14}N(**D**) atoms. Therefore, the nonbonding electrons of these atoms dominantly determine the q_{ZZ} values and thus increase the NQCC values. The larger values of the inter-atomic distances in Gly–Leu dimer also confirm this point.

D) The ^{14}N nucleus is one of the most important quadrupolar nuclei in peptides. The data in Table 3 show that in monomers, the ^{14}N NQCC is insensitive to the change of the R group. This implies that the interaction between R and this nitrogen atom is rather weak. This could be expected as the ^{14}N nucleus is shielded effectively by its three bonded groups, as contrasted to the ^{2}D and ^{17}O nuclei. In dimers, however, the ^{14}N NQCC value slightly increases with the increase in the size

Table 7
The optimized values of inter-atomic distances R_{i-j} (in Å) and dihedral angles $D_{i-j-k-l}$ (in degrees) corresponding to the ^{17}O(**C**) and ^{14}N(**D**) atoms obtained for amino acid dimers using MP2/6-311++G** method

R_{i-j}	Gly–Gly	Gly–Ala	Gly–Val	Gly–Ile	Gly–Leu
R_{1-2}	1.4777	1.4787	1.4793	1.4776	1.4777
R_{1-3}	1.7759	1.7885	1.8147	1.7946	1.7902
R_{3-4}	0.9925	0.9915	0.9908	0.9893	0.9896
R_{4-5}	1.3365	1.3383	1.3400	1.3378	1.3372
R_{2-4}	3.6376	3.6505	3.6983	3.6548	3.6718
R_{1-5}	3.4668	3.4751	3.4620	3.4859	3.4514
R_{2-5}	3.8600	3.8691	3.8780	3.8831	3.8641
$D_{i-j-k-l}$	Gly–Gly	Gly–Ala	Gly–Val	Gly–Ile	Gly–Leu
$D_{3-4-5-6}$	3.6	0.4	4.8	0.8	4.7
$D_{4-5-6-7}$	65.0	71.0	77.7	69.1	76.4
$D_{4-5-6-8}$	5.4	13.3	21.4	15.4	18.7
$D_{9-5-6-8}$	6.0	14.7	23.8	16.3	20.3
$D_{9-5-6-7}$	65.6	72.3	80.1	70.0	77.9

See Fig. 5 for numbering scheme.

of the R group. It means that the interaction between the R group and this nitrogen atom in dimers can not be totally neglected.

E) The ^{2}D NQCC of the hydrogen atoms of the terminal amino group in monomers decreases versus increasing the size of the R group. This indicates the greater interaction between larger R groups and these hydrogen atoms. While in the dimers, variation in the ^{2}D NQCC value is not considerable. In peptides, hydrogen atoms of the amino group and oxygen atom of the carboxylic group interact effectively through hydrogen bonding. Therefore, ^{2}D NQCC study of these amino deuterons without considering the hydrogen bond interaction results in unrealistic conclusions. The hydrogen bond geometry has been reported to have a close relationship with the ^{2}D NQCC of N–^{2}D of the end amino group in the peptide so that, the ^{2}D NQCC is decreased as deuterium atom is involved in a stronger hydrogen bond [51,52].

F) Similar to H_{α}, the calculated value of NQCC for ^{2}D of the peptide bond decreases with the size of the R group. Also, increasing the size of the R group increases the N–H bond length of the peptide group. In other words, the interaction between R and H causes a decrease in the electron density between N and H in peptide bond and therefore, N–H bond length increases. The results presented in Table 5 confirm this analysis.

G) No well-defined variation with the size of the R group has been observed for the NQCC values of the ^{14}N and ^{17}O nuclei belonging to the peptide bond. Also, no correlation could be established between the calculated ^{14}N and ^{17}O NQCC values and the C⌒O and C–N bond lengths.

4. Conclusions

The ^{2}D, ^{14}N and ^{17}O nuclear quadrupole coupling constants for aliphatic amino acids and their dimers have been calculated. A correlation has been found between these calculated coupling constants and conformational structures of the aliphatic amino acid monomers and dimers.

For small amino acids studied here, such as glycine, the ^{2}D NQCC values in the gas phase can be confidently evaluated (and compared with experimental data) by using Møller–Plesset second-order perturbation theory method. Variation of the NQCC values on going from the gas phase to the solid state can be reasonably well reproduced at a qualitative level by using a suitable basis set.

Asymmetry parameters, however, are difficult to be reproduced with accuracy. Calculated values of asymmetry parameters are much affected by small changes in any of the involved components of the EFG tensor caused by small changes in the chemical environment (whether via the direct chemical bonds or through space) of the quadrupolar nuclei.

The calculated values of the ^{17}O NQCC for the terminal carboxylic group have the least variation (less than 2.5%) for monomers and less than 4.5% for dimers with the change in the size of the R residue. While, the calculated values of the ^{14}N NQCC for the terminal amino group in the amino acid dimers have the greatest variation (about 8%) with the change in the size of the R residue.

Different residues R, on a given amino acid monomer or dimer do not significantly affect the NQCC parameter of the nuclei of the peptide group atoms.

The NQCC parameters of the selected molecules are dependent on the particular conformation of the residues, specifically on the value of the dihedral angles.

Computationally predicted NQCC data, like the ones reported here, can be confidently used to elucidate the components of the EFG tensor of larger peptides, such as trimers and tetramers, and to determine that the NQCC of which group can truly be considered as a characteristic physical property.

The characteristic factors in NQR spectroscopy are quadrupole moments and EFG's. Asymmetric charge distribution around the quadrupole nuclei results in EFG. However, in solution, the EFG is symmetric due to the random tumbling (with the change of orientation) of solute and solvent molecules, and consequently, the q_{ZZ} vanishes (similar to what observed for dipole–dipole interaction in liquid NMR spectroscopy). Therefore, solvent effects have no significant role in the NQR measurements as no signal is observed for liquid samples. This is while solvent effects have a major role in the other spectroscopic techniques such as NMR and IR. All NQR parameters reported in literature are measured either in the solid or gas phase [19]. It should be noted however that for the solvents having strong interaction with solutes and thus altering its optimized structure, solvent effect on the NQCC parameter should be taken into consideration. Furthermore, all of the quantum mechanical computations carried out in this work are applicable to isolated gas phase species only, which is intended in this research.

The results of this study shows that NQR method can be used effectively as a complement method in the situations where other spectroscopic methods are difficult to apply or their results are associated with large uncertainties.

Acknowledgment

We acknowledge Prof. F.R.W. McCourt of UW for allowing us to use their software and hardware facilities via Internet. Supports of Tarbiat Modares University and the University of Isfahan as research facilities are also appreciated.

References

[1] K. Coutinho, S. Canuto, M.C. Zerner, Calculation of the absorption spectrum of benzene in condensed phase. A study of the solvent effect, J. Quant. Chem. 65 (1997) 885–891.
[2] M. Karelson, M.C. Zerner, Theoretical treatment of solvent effects on electronic spectroscopy, J. Phys. Chem. 96 (1992) 6949–6957.
[3] W.-G. Han, K.J. Jalkanen, M. Elstner, S. Suhai, Theoretical study of aqueous *N*-acetyl(-L-alanine *N*′-mathylamide: structures and Raman, VCD, and ROA spectra, J. Phys. Chem., B 102 (1998) 2587–2602.
[4] T.A. Cross, J.R. Quine, Protein structure in anisotropic environments: development of orientational constraints, Concepts Magn. Reson. 12 (2000) 55–70.
[5] K. Schmidt-Rohr, H.W. Spiess, Multi-dimensional Solid-State NMR and Polymers, Academic Press, London, 1999.
[6] R.R. Ketchem, W. Hu, T.A. Cross, High-resolution conformation of gramicidin A in a lipid bilayer by solid-state NMR, Science 261 (1993) 1457–1460.

[7] R.R. Ketchem, K.C. Lee, S. Huo, T.A. Cross, Macromolecular structural lucidation with solid-state NMR-derived orientational constraints, J. Biomol. NMR 8 (1996) 1–14.
[8] M. Cotten, V.G. Soghomonian, W. Hu, T.A. Cross, High resolution and high field in biological solid state NMR, Solid State NMR 9 (1997) 77–80.
[9] A. Watts, I.J. Burnett, C. Glaubitz, G. Gröbner, D.A. Middleton, P.J.R. Spooner, J.A. Watts, P.T.F. Williamson, Membrane protein structure determination by solid state NMR, Nat. Prod. Rep. 16 (1999) 419–423.
[10] J. Wang, J. Denny, C. Tian, S. Kim, Y. Mo, F. Kovacs, Z. Song, K. Nishimura, Z. Gan, R. Fu, J.R. Quine, T.A. Cross, Imaging membrane protein helical wheels, J. Magn. Reson. 144 (2000) 162–167.
[11] M. Hong, R.G. Griffin, Resonance assignments for solid peptides by dipolar-mediated $^{13}C/^{15}N$ correlation solid-state NMR, J. Am. Chem. Soc. 120 (1998) 7113–7114.
[12] F.M. Marassi, J.J. Gesell, A.P. Valente, Y. Kim, M. Oblatt-Montal, M. Montal, S.J. Opella, Dilute spin-exchange assignment of solid-state NMR spectra of oriented proteins: acetylcholine M2 in bilayers, J. Biomol. NMR 14 (1999) 141–148.
[13] C.H. Wu, A. Ramamoorthy, S.J. Opella, High-resolution heteronuclear dipolar solid-state NMR spectroscopy, J. Magn. Reson., A 109 (1994) 270–274.
[14] J.D. Graybeal, Molecular Spectroscopy, McGraw-Hill, Singapore, 1988.
[15] M.H. Cohen, F. Reif, Quadrupole effects in nuclear magnetic resonance studies of solids, Solid State Phys. 5 (1957) 321–438.
[16] L. Hemmingsen, U. Ryde, Ab initio calculation of electric field gradients in cadmium complexes, J. Phys. Chem. 100 (1996) 4803–4809.
[17] T.K. Ha, M.J. Kellr, R. Gunde, H.H. Gunthard, Quantum chemical study of structure, energy, rotational constants, electric dipole moments and electric field gradients of all isomeric adenines, J. Mol. Struct. 364 (1996) 161–181.
[18] M. Torrent, D. Mansour, E.P. Day, K. Morokuma, Quantum chemical study on oxygen-17 and nitrogen-14 nuclear quadrupole coupling parameters of peptide bonds in α-helix and β-sheet proteins, J. Phys. Chem., A 105 (2001) 4546–4557.
[19] E.A.C. Lucken, Nuclear Quadrupole Coupling Constants, Academic Press, London, 1969.
[20] M.J. Frisch, G.W. Trucks, H.B. Schlegel, G.E. Scuseria, M.A. Robb, J.R. Cheeseman, V.G. Zakrzewski, J.A. Montgomery Jr., R.E. Stratmann, J.C. Burant, S. Dapprich, J.M. Millam, A.D. Daniels, K.N. Kudin, M.C. Strain, O. Farkas, J. Tomasi, V. Barone, M. Cossi, R. Cammi, B. Mennucci, C. Pomelli, C. Adamo, S. Clifford, J. Ochterski, G.A. Petersson, P.Y. Ayala, Q. Cui, K. Morokuma, D.K. Malick, A.D. Rabuck, K. Raghavachari, J.B. Foresman, J. Cioslowski, J.V. Ortiz, A.G. Baboul, B.B. Stefanov, G. Liu, A. Liashenko, P. Piskorz, I. Komaromi, R. Gomperts, R.L. Martin, D.J. Fox, T. Keith, M.A. Al-Laham, C.Y. Peng, A. Nanayakkara, C. Gonzalez, M. Challacombe, P.M.W. Gill, B. Johnson, W. Chen, M.W. Wong, J.L. Andres, C. Gonzalez, M. Head-Gordon, E.S. Replogle, J.A. Pople, Gaussian 98, Gaussian Inc, Pittsburgh PA, 1998.
[21] K.D. Sen, Reviews of Modern Quantum Chemistry, World Scientific, Singapore, 2002.
[22] Y. Ding, K. Krogh-Jespersen, The glycine zwitterion does not exist in the gas phase: results from a detailed ab initio electronic structure study, Chem. Phys. Lett. 199 (1992) 261–266.
[23] D. Yu, D.A. Armstrong, A. Rauk, Hydrogen bonding and internal rotation barriers of glycine and its zwitterion (hypothetical) in the gas phase, Can. J. Chem. 70 (1992) 1762–1772.
[24] S. Gronert, R.A.J. O'Hair, Ab initio studies of amino acid conformations. 1. The conformers of Alanine, Serine, and Cysteine, J. Am. Chem. Soc. 117 (1995) 2071–2081.
[25] A.G. Csaszar, Conformers of gaseous α-alanine, J. Phys. Chem. 100 (1996) 3541–3551.
[26] H.A. Levy, R.B. Corey, The crystal structure of dl-alanine, J. Am. Chem. Soc. 63 (1941) 2095–2108.
[27] M.S. Lehmann, T.F. Koetzle, N.C. Hamilton, Precise neutron diffraction structure determination of protein and nucleic acid components I. crystal and molecular structure of the amino acid L-alanine, J. Am. Chem. Soc. 94 (1972) 2657–2660.
[28] H.A. Levy, R.B. Corey, The crystal structure of DL-alanine, J. Am. Chem. Soc. 63 (1941) 2059–2062.
[29] J. Donohue, The crystal structure of DL-alanine. II. Revision of parameters by three-dimensional Fourier analysis, J. Am. Chem. Soc. 72 (1950) 949–953.
[30] J.H. Davis, The description of membrane lipid conformation, order and dynamics by ^{2}H-NMR, Biochim. Biophys. Acta 737 (1983) 117–171.
[31] J.H. Davis, in: E. Buncel, J.R. Jones (Eds.), Isotopes in the Physical and Biophysical Sciences, vol. 2, Elsevier, Amsterdam, 1991.
[32] J.H. Davis, in: L. Finegold (Ed.), Cholesterol in Membrane Models, CRC Press, Boca Raton, Florida, 1993.
[33] P. Pyykko, Spectroscopic nuclear quadrupole moments, Mol. Phys. 99 (2001) 1617–1629.
[34] A.C. LiWang, Ad. Bax, Solution NMR characterization of hydrogen bonds in a protein by indirect measurement of deuterium quadrupole couplings, J. Magn. Reson. 127 (1997) 54–64.
[35] S. Mukherjee, S. Majumdar, D. Bhattacharyya, Role of hydrogen bonds in protein–DNA recognition: effect of nonplanar amino groups, J. Phys. Chem., B 109 (2005) 10484–10492.
[36] R. Wieczorek, J.J. Dannenberg, Hydrogen-bond cooperativity, vibrational coupling, and dependence of helix stability on changes in amino acid sequence in small 310-helical peptides. A Density Functional Theory Study, J. Am. Chem. Soc. 125 (2003) 14065–14071.
[37] M. Strohmeier, D. Stueber, D.M. Grant, Accurate ^{13}C and ^{15}N chemical shift and ^{14}N quadrupolar coupling constant calculations in amino acid crystals: zwitterionic, hydrogen-bonded systems, J. Phys. Chem., A 107 (2003) 7629–7642.
[38] S. Scheiner, T. Kar, J. Pattanayak, Comparison of various types of hydrogen bonds involving aromatic amino acids, J. Am. Chem. Soc. 124 (2002) 13257–13264.
[39] E. Tajkhorshid, K.J. Jalkanen, S. Suhai, Structure and vibrational spectra of the zwitterions L-alanine in the presence of explicit water molecules: a density functional analysis, J. Phys. Chem., B 102 (1998) 5899–5913.
[40] V. Lemaitre, M.E. Smith, A. Watts, A review of oxygen-17 solid-state NMR of organic materials—towards biological applications, Solid State Nucl. Magn. Reson. 26 (2004) 215–235.
[41] K.J. Pike, V. Lemaitre, A. Kukol, T. Anupold, A. Samoson, A.P. Howes, A. Watts, M.E. Smith, R. Dupree, Solid-state ^{17}O NMR of amino acids, J. Phys. Chem., B 108 (2004) 9256–9263.
[42] J. Seliger, ^{17}O quadrupole coupling in C–O–H...O⌒C hydrogen bond, Chem. Phys. 231 (1998) 81–86.
[43] J. Seliger, V. Zagar, R. Blinc, A. Novak, ^{17}O and ^{39}K quadrupole resonance study of the ferroelastic phase transition in $KH_3(SeO_3)_2$, J. Chem. Phys. 84 (1986) 5857–5861.
[44] I.J.F. Poplett, J.A.S. Smith, Oxygen-17 and deuterium quadrupole double resonance in some carboxylic acid dimers, J. Chem. Soc., Faraday Trans. 277 (1981) 1473–1485.
[45] J.P. Foster, F. Weinhold, Natural hybrid orbitals, J. Am. Chem. Soc. 102 (1980) 7211–7218.
[46] A.E. Reed, F. Weinhold, Natural bond orbital analysis of near-Hartree-Fock water dimer, J. Chem. Phys. 78 (1983) 4066–4073.
[47] A.E. Reed, R.B. Weinstock, F. Weinhold, Natural population analysis, J. Chem. Phys. 83 (1985) 735–746.
[48] J.E. Carpenter, F. Weinhold, Analysis of the geometry of the hydroxymethyl radical by the "different hybrids for different spins" natural bond orbital procedure, J. Mol. Struct., Theochem 169 (1988) 41–62.
[49] A.E. Reed, F. Weinhold, Natural bond orbital analysis of near-Hartree-Fock water dimmer, J. Chem. Phys. 78 (1983) 4066–4073.
[50] A.E. Reed, L.A. Curtiss, F. Weinhold, Intermolecular interactions from a natural bond orbital, donor-acceptor viewpoint, Chem. Rev. 88 (1988) 899–926.
[51] L.G. Butler, T.L. Brown, Nuclear quadrupole coupling constants and hydrogen bonding. Molecular orbital study of oxygen-17 and deuterium field gradients in formaldehyde-water hydrogen bonding, J. Am. Chem. Soc. 103 (1981) 6541–6549.
[52] M.J. Hunt, A.L. Mackay, Deuterium and nitrogen pure quadrupole resonance in deuterated amino acids, J. Magn. Reson. 22 (1976) 295–301.